PLOS ONE

RESEARCH ARTICLE

ZBTB38 is dispensable for antibody responses

Rachel Wong[1,2], **Deepta Bhattacharya**[2]*

1 Division of Biological and Biomedical Sciences, Washington University in St. Louis, Saint Louis, MO, United States of America, **2** Department of Immunobiology, University of Arizona, Tucson, AZ, United States of America

* deeptab@email.arizona.edu

OPEN ACCESS

Citation: Wong R, Bhattacharya D (2020) ZBTB38 is dispensable for antibody responses. PLoS ONE 15(9): e0235183. https://doi.org/10.1371/journal.pone.0235183

Editor: Yolande Richard, Institut Cochin, FRANCE

Received: June 9, 2020

Accepted: September 7, 2020

Published: September 21, 2020

Data Availability Statement: RNA-seq data have been deposited at NCBI GEO GSE 152109. All other data are within the manuscript and Supporting Information files.

Funding: This work was supported by National Institutes of Health (https://www.niaid.nih.gov/) grant R01AI099108 (D.B.). R.W. was supported by the National Science Foundation (https://www.nsfgrfp.org/) Graduate Research Fellowship Program (DGE-1143954). The funders had no role in study design, data collection and analysis, decision to publish, or preparation of the manuscript.

Abstract

Members of the broad complex, tram track, bric-a-brac and zinc finger (BTB-ZF) family of transcription factors, such as BCL-6, ZBTB20, and ZBTB32, regulate antigen-specific B cell differentiation, plasma cell longevity, and the duration of antibody production. We found that ZBTB38, a different member of the BTB-ZF family that binds methylated DNA at CpG motifs, is highly expressed by germinal center B cells and plasma cells. To define the functional role of ZBTB38 in B cell responses, we generated mice conditionally deficient in this transcription factor. Germinal center B cells lacking ZBTB38 dysregulated very few genes relative to wild-type and heterozygous littermate controls. Accordingly, mice with hematopoietic-specific deletion of *Zbtb38* showed normal germinal center B cell numbers and antibody responses following immunization with hapten-protein conjugates. Memory B cells from these animals functioned normally in secondary recall responses. Despite expression of ZBTB38 in hematopoietic stem cells, progenitors and mature myeloid and lymphoid lineages were also present in normal numbers in mutant mice. These data demonstrate that ZBTB38 is dispensable for hematopoiesis and antibody responses. These conditional knockout mice may instead be useful in defining the functional importance of ZBTB38 in other cell types and contexts.

Introduction

Antibody responses following infections or vaccinations are initiated by a series of B cell activation steps and fate decisions [1]. Upon recognition of cognate antigens and other stimulatory signals, B cells grow in size, express a panel of activation markers, begin to proliferate, and a subset undergoes immunoglobulin isotype-switching [2]. In T cell-dependent responses, B cells then differentiate either into antibody-secreting plasma cells or into germinal center B cells. Germinal centers are the sites in which somatic hypermutation and affinity maturation occur and are under substantial replicative and DNA damage-induced stress. Germinal centers eventually produce long-lived plasma cells (LLPCs) and memory B cells (MBCs), which have distinct antigen specificities and mediate different aspects of immunity [3]. LLPCs constitutively secrete antibodies and are important for providing protection against re-infection by the same pathogen. Memory B cells, on the other hand, can only provide protection after re-activation by a cognate antigen through rapid differentiation into plasma cells or secondary

Competing interests: Sana Biotechnology has licensed intellectual property of D.B. R.W. has no competing interests. This does not alter our adherence to PLoS ONE policies on sharing data and materials.

germinal center B cells. Recent studies have identified the broad complex, tram track, bric-a-brac and zinc finger (BTB-ZF) family of transcription factors as key regulators in B cell development. BTB-ZF family members bind DNA through its C-terminal zinc finger domains and recruit SMRT co-repressors and histone deacetylases to N-terminal BTB/POZ domains [4–8]. Family members that regulate distinct aspects of B cell-mediated immunity include BCL-6, ZBTB20, and ZBTB32. BCL-6 is important for germinal center (GC) formation [9], ZBTB20 promotes plasma cell lifespan and durable immunity in an adjuvant dependent manner [10, 11], and ZBTB32 restricts memory B cell recall responses [12, 13]. Other as-yet uncharacterized BTB-POZ members may regulate different aspects of B cell responses [4].

ZBTB38, also known as CIBZ (CtBP-interacting BTB zinc finger protein), is another member of the BTB-ZF family and can function either as a transcriptional repressor or activator [14]. In contrast to other BTB-ZF factors that bind to similar DNA sequences, ZBTB38-mediated transcriptional regulation occurs by binding primarily to specific methylated CpG sequences and recruiting repressors or activators [15–19]. The uniqueness of ZBTB38 binding sites relative to other BTB-POZ factors led us to speculate that this factor would have a functionally important and non-redundant role in B cell responses. Indeed, ZBTB38 has been shown to repress overall transcription by inhibiting expression of MCM10, a component of the pre-replication complex [20]. Additionally, ZBTB38 can, directly or indirectly, regulate cell cycle progression, cellular differentiation, and apoptosis [21–25]. In contrast to this speculation, we demonstrate that, despite high levels of expression in germinal center B lymphocytes and plasma cells, ZBTB38 deficiency does not impair primary or secondary antibody responses to T cell-dependent model immunogens.

Materials and methods

Ethics statement

All procedures in this study were specifically approved and carried out in accordance with the guidelines set forth by the Institutional Animal Care and Use Committee at Washington University (approval 20140030) and at the University of Arizona (approval 17–266). Euthanasia was performed by administering carbon dioxide at 1.5L/minute into a 7L chamber until 1 minute after respiration ceased. After this point, cervical dislocation was performed to ensure death.

Mice

All mice were housed and bred in pathogen-free facilities. C57BL6/N mice were obtained from the National Cancer Institute. B6.Cg-*Igh*^{a}*Thy1*^{a}*Gpi1*^{a} (*IgH*^{a}) mice were obtained from Charles River Laboratories. *Zbtb38*$^{fl/+}$ mice were generated by injecting C57Bl6/J pronuclear zygotes with ribonucleoparticles of Cas9 protein and guide RNAs targeting sites flanking exon 3 of *Zbtb38*, alongside oligonucleotide donors as homologous recombination donors spanning these same gRNA sites. Oligonucleotide substrates contained loxP sites to interrupt gRNA target sites to prevent Cas9 re-cutting after successful recombination. A single successful founder (out of 33 tested) was identified by PCR and then bred to C57Bl6/N mice for germline transmission. Mice have been maintained by backcrossing to C57Bl6/N animals. Animals will be made available at the Mutant Mouse Resource and Research Centers upon publication of this manuscript (B6N.B6J-*Zbtb38em1Dbhat*/Mmucd, Strain ID 66871). ZBTB38 f/f mice were crossed to CMV-Cre (Jackson Laboratory, stock no. 006054) or VavCre (Jackson Laboratory, stock no. 008610) and maintained as ZBTB38 f/f or ZBTB38 x CMV- or Vav-Cre where littermates were used as controls. The following primers were used to confirm recombination of the targeting plasmid: SP55.mZbtb38.5'genomic.F2 `5′- CCAGGGATTCAGTCCTCAGCA-3′`,

SP55.mZbtb38.3'genomic.R2 5′- GCCTACCCCAAACCACACTAA-3′. The following primers were used for genotyping the *Zbtb38* allele: 5'LoxP forward 5′- TCTGAGTTCAAGGCCA GCTT-3′, 5'LoxP reverse 5′- TCTCCAAGCAGAAAGGGTGT-3′, and 3'LoxP reverse 5′- GGGTCGTTAGAGGATTCAGC-3′.

Immunizations

Mice were immunized intraperitoneally with 100 μg NP-OVA (Biosearch), adjuvanted with Alhydrogel (Invivogen). NP-APC used for staining was made by conjugating allophycocyanin (Sigma-Aldrich) with 4-hydroxy-3-nitrophenylacetyl-O-succinimide ester (Biosearch Technologies).

RNA extraction, cDNA synthesis, and qRT-PCR

Total RNA was extracted with TRIzol (Life technologies) and cDNA synthesized using Superscript III Reverse transcription kit with random hexamers (Life Technologies) according to manufacturer's instructions. qRT-PCR was performed using SYBR Green PCR master mix (Applied Biosystems) on a Prism 7000 Sequence Detection System (Applied Biosystems). The primers used for *Zbtb38* are: forward 5′- AGAACCAAGGATTTCCGAGTG-3′ and reverse 5′-GATGGAGAGTACTGTGTCACTG-3′. *Zbtb38* transcript levels were normalized to 18S ribosomal RNA, forward 5′-CGGCTACCACATCCAAGGAA-3′ and reverse 5′-GCTGG AATTACCGCGGCT-3′ [26].

RNA-sequencing

RNA from germinal center B cells was extracted with Macherey-Nagel Nucleospin XS kits. cDNA libraries were prepared by Novogene using SmartSeq v4 kits (Takara) and processed for paired-end PE150 RNA-sequencing on an Illumina Hiseq 4000 lane. For visualization of ZBTB38 transcripts, fastq files were mapped and aligned to the mm10 genome using HiSat2 and displayed using IgV [27, 28]. For quantification of gene expression differences, fastq files were mapped using vM17 annotation files from Gencode and transcript abundances were quantified by Salmon [29]. Differentially-expressed genes quantified by DESeq2 [30]. Volcano plots were displayed using Prism software (GraphPad). Data is available on NCBI GEO (GSE152109).

ELISA

ELISA plates (9018, Corning) were coated overnight at 4˚C in 0.1 M sodium bicarbonate buffer, pH 9.5 containing 5 ug/mL of NP_{16}- or NP_4-BSA (Bioresearch Technologies). All other incubation steps were performed at room temperature for 1 hour. Wash steps were performed between each step using PBS + 0.05% Tween-20. Plates were blocked with PBS + 2% BSA followed by serial dilutions of serum. Serum was probed with 0.1 ug/mL of biotinylated anti-mouse IgG (715-065-151, Jackson ImmunoResearch Laboratories) and then detected with streptavidin conjugated horseradish peroxidase (554066, BD biosciences). Plates were developed using TMB (Dako, S1599) and neutralized with 2N H_2SO_4. Optical density (OD) values were measured at 450 nm. Serum endpoint titer was defined as the inverse dilution factor that is three standard deviations above background using one-phase decay measurements and Prism software (GraphPad Software).

Adoptive transfer for recall responses

Splenocytes from NP-immunized *ZBTB38*$^{f/f}$ or *ZBTB38*$^{f/f}$ x VavCre mice were isolated and processed into single cell suspension, erythrocytes lysed using an ammonium chloride-

potassium solution, and lymphocytes isolated by using a Hisopaque-1119 (Sigma-Aldrich) density gradient. Cells were washed twice prior to transfer. 10% of cells were retained for cellular analysis whereas the remaining 90% of cells were transferred into one non-irradiated IgH^a recipient mice by intravenous injection. A recall response was elicited by intravenously challenging mice with soluble NP-OVA 24 hours later.

Flow cytometry

Single cell suspensions were prepared from bone marrow or spleen, erythrocytes lysed using an ammonium chloride-potassium solution, and lymphocytes isolated by using a Hisopaque-1119 (Sigma-Aldrich) density gradient. Cells were resuspended in PBS with 5% adult bovine serum and 2 mM EDTA prior to staining with antibodies and NP-APC. The following antibodies were purchased from Biolegend: 6D5 (CD19)-Alexa Fluor 700; GL7-FITC; 281–2 (CD138)-PE; RMM-1 (IgM)-APC; 11-26c.2a (IgD)-PerCP-Cy5.5 or -Brilliant Violet 605; 16-10A1 (CD80)-PE; RA3-6B2 (B220)-FITC, -Pacific Blue, or APC-Cy7; PO3 (CD86)-FITC; PK136 (NK-1.1)-PerCP-Cy5.5; M1/70 (CD11b)-Pacific Blue; HK1.4 (Ly-6C)-Brilliant Violet 510; 1A8 (Ly-6G)-Brilliant Violet 605; A7R34 (IL-7R)-Brilliant Violet 421; E13-16.7 (Ly-6A/E)-PE; and 29-2L17 (CCR6)-PE-Cy7. The following antibodes were purchased from eBioscience: 11/41 (IgM)-PerCP-e710; 11-26c (IgD)-FITC; 2B11 (CXCR4)-PerCP-e710; 2B8 (c-Kit)-PE-Cy7; and LG.7F9 (CD27)-APC. The following antibodies were purchased from BD Pharmingen: 53–6.7 (CD8a)-PE; RM4-5 (CD4)-PE-Cy7; A2F10.1 (CD135)-PE-CF594; and 93 (CD16/CD32)-PerCP-Cy5.5.

Cells were stained on ice for 20 minutes. Germinal center B cells were enriched by staining cells with GL7-PE followed with anti-PE magnetic beads (0.5 uL/10^7 cells, Miltenyi Biotec). Positive enrichment of GL7-expressing cells was performed using MACS LS columns (Miltenyi Biotec).

Statistical analysis

Statistical analyses were performed using GraphPad Prism 8. Specific tests used, and significance, is indicated in each panel.

Results

ZBTB38 is highly expressed in B cell subsets

RNA-sequencing studies have reported expression of ZBTB38 in plasma cells [31]. To look more broadly across hematopoietic lineages, ZBTB38 gene expression in multiple cell types was first analyzed using available RNA-sequencing data assembled by the ImmGen Consortium [32]. A subset of cell types expressing DESeq2-normalized ZBTB38 counts greater than 800 are shown in Fig 1A [30]. High expression of ZBTB38 was observed in splenic plasma cells and plasmablasts (PC and PB), and in both light zone and dark zone germinal center B cells (LZ and DZ, Fig 1A). To confirm these data, wild-type mice were immunized with alhydrogel-adjuvanted 4-hydroxy-3-nitrophenyl-acetyl (NP) conjugated to ovalbumin (OVA) and naïve B cells ($CD19^+CD138^-GL7^-IgD^+$), NP-specific dark ($CXCR4^+$) and light zone ($CD86^+$) GC B cells ($CD19^+GL7^+IgD^-$), and NP-specific splenic plasma cells ($CD138^+$) were sorted 11 days after immunization [33]. RNA was extracted from sorted cells and quantitative RT-PCR performed to quantify ZBTB38 transcript levels. GC B cells and splenic plasma cells contained 9- and 3-fold, respectively, higher expression of ZBTB38 compared to naïve B cells (Fig 1B; S1 Fig). We further confirmed these findings by examining published microarray data on dark and light zone GCs [33]. Both GC subsets expressed 3–4 fold higher levels of ZBTB38 than did

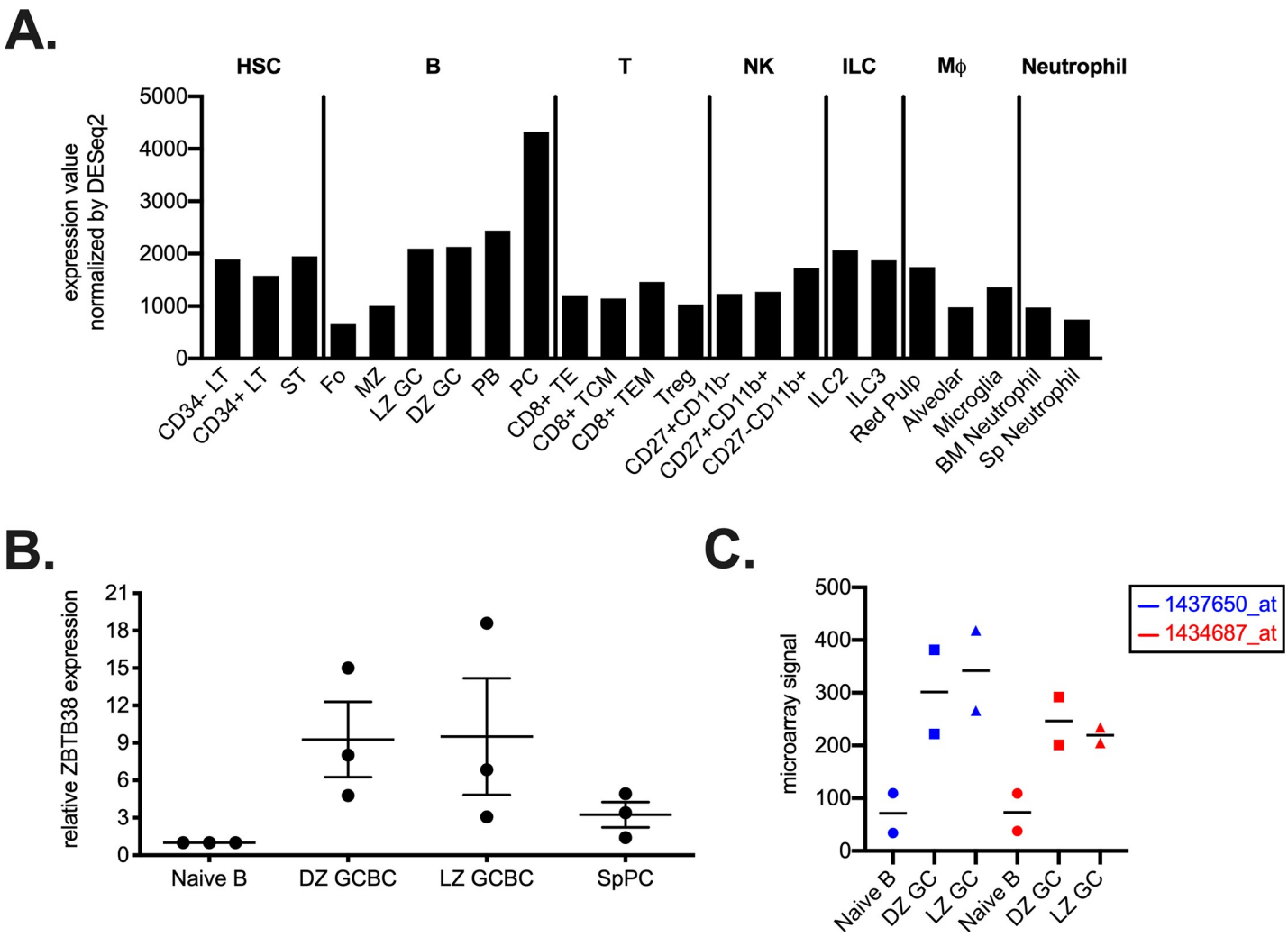

Fig 1. ZBTB38 is highly expressed by specific hematopoietic lineages. (**A**) ZBTB38 expression values in select cell subsets with DESeq2 count values over 800 were extracted from ImmGen's RNA-seq SKYLINE and grouped based on cell type. (**B**) Naïve B cells ($CD19^+CD138^-GL7^-IgD^+$), antigen-specific (NP^+) dark (DZ, $CXCR4^+$) and light (LZ, $CD86^+$) zone germinal center B cells (GC, $CD19^+GL7^+IgD^-$), and splenic plasma cells (SpPC, $CD138^+$) were sorted 11 days after immunization of C57BL/6 mice with NP-OVA in alhydrogel, and *Zbtb38* RNA levels quantified by quantitative RT- PCR. ZBTB38 expression was first normalized to 18S expression level followed by normalization to naïve B cells. Gating strategies are shown in S1 Fig. Mean ± SEM are shown; each symbol represents an individual mouse. (**C**) Microarray quantification from two different probesets (blue and red symbols) of ZBTB38 expression across DZ, LZ, and naïve B cells [33]. Data were normalized and obtained from NCBI GEO2R.

https://doi.org/10.1371/journal.pone.0235183.g001

naïve B cells across two probesets (Fig 1C). No differences in ZBTB38 expression were observed between light and dark zone GC B cells.

Generation and validation of ZBTB38 conditional knockout mice

To assess the functional role of ZBTB38 *in vivo*, we generated *Zbtb38* floxed mice by targeting exon 3 (Fig 2A). This terminal exon contains the entire protein-coding sequence of ZBTB38. Single-stranded oligonucleotides containing loxP sites and flanking sequences of exon 3 of *Zbtb38* were microinjected alongside Cas9/guideRNA ribonucleoparticles into C57Bl6/J zygotes. gRNA sites were designed to flank the endogenous *Zbtb38* exon 3 and be disrupted upon homologous recombination with the targeting oligonucleotides. NdeI and EcoRI restriction sites were included in the oligonucleotides near the 5' LoxP and 3' LoxP sites to screen for

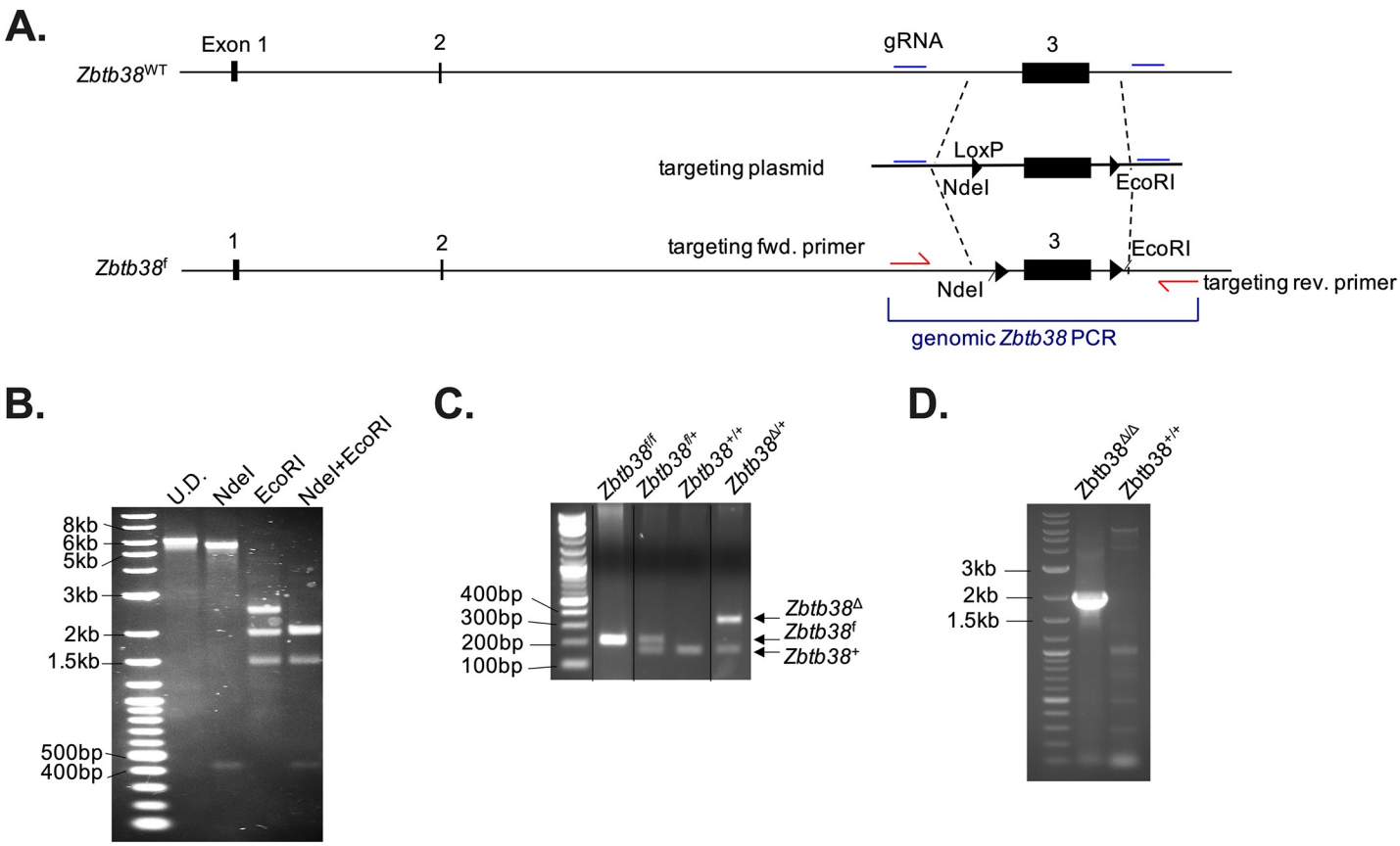

Fig 2. *Zbtb38* targeting strategy and confirmation of deletion. (A) Targeting strategy for exon 3 of *Zbtb38*. Guide RNA (gRNA) sites and targeting single-stranded oligonucleotides containing NdeI and EcoRI restriction sites were introduced to allow for screening of homologous recombination. **(B)** PCR strategy for exon 3 to confirm correct targeting. Lane 1 shows undigested PCR product, lane 2 shows NdeI digest (expected band sizes of 5.8 kb and 445 bp), lane 3 shows EcoRI digest (expected band sizes of 2.6 kb, 2 kb, and 1.6 kb), and lane 4 shows NdeI and EcoRI double digest (expected band sizes of 445 bp, 2.1 kb, 2 kb, and 1.6 kb). **(C)** Genotyping strategy and results to identify WT, floxed, or deleted *Zbtb38* alleles. **(D)** PCR confirming Zbtb38 deletion upon Cre expression. Primers used are identical to those used to amplify the genomic DNA as in **(B)**, but a shorter extension time was used.

https://doi.org/10.1371/journal.pone.0235183.g002

successful homologous recombination of the targeting construct. Correct targeting of exon 3 was confirmed by PCR and restriction enzyme digestions (Fig 2B). Wild-type, targeted, and *Zbtb38*-deleted mice were distinguished using a set of three PCR primers flanking the 5' and 3' LoxP sequences (Fig 2C). To confirm deletion of *Zbtb38* exon 3 at the genomic level, *Zbtb38* f/f mice were crossed to mice expressing CMV-Cre to obtain germline ZBTB38 deletion. Tail genomic DNA from *Zbtb38* f/f x CMV-Cre was amplified and deletion was confirmed by a 4 kb reduction in PCR amplicon size (Fig 2D). Despite genome-wide association studies linking polymorphisms in the *Zbtb38* locus to human height [34–36], no differences were observed in the size of ZBTB38 deficient vs. wild-type littermates, and animals were born in expected Mendelian ratios.

Given the high expression of ZBTB38 in blood lineages, we crossed *Zbtb38* f/f mice to VavCre mice (*Zbtb38* f/f x VavCre, ZBTB38 KO), which express Cre recombinase primarily in hematopoietic cells [37]. To confirm loss of ZBTB38 expression in this system, we performed RNA-seq on germinal center B cells isolated 2 weeks after immunization with NP-OVA. After mapping reads and aligning to the mouse genome, we observed that transcripts within the floxed exon 3 were completely abrogated in ZBTB38 KO mice, whereas intermediate levels were observed in *Zbtb38* f/+ x VavCre heterozygous littermates (Fig 3A) relative to *Zbtb38* f/f

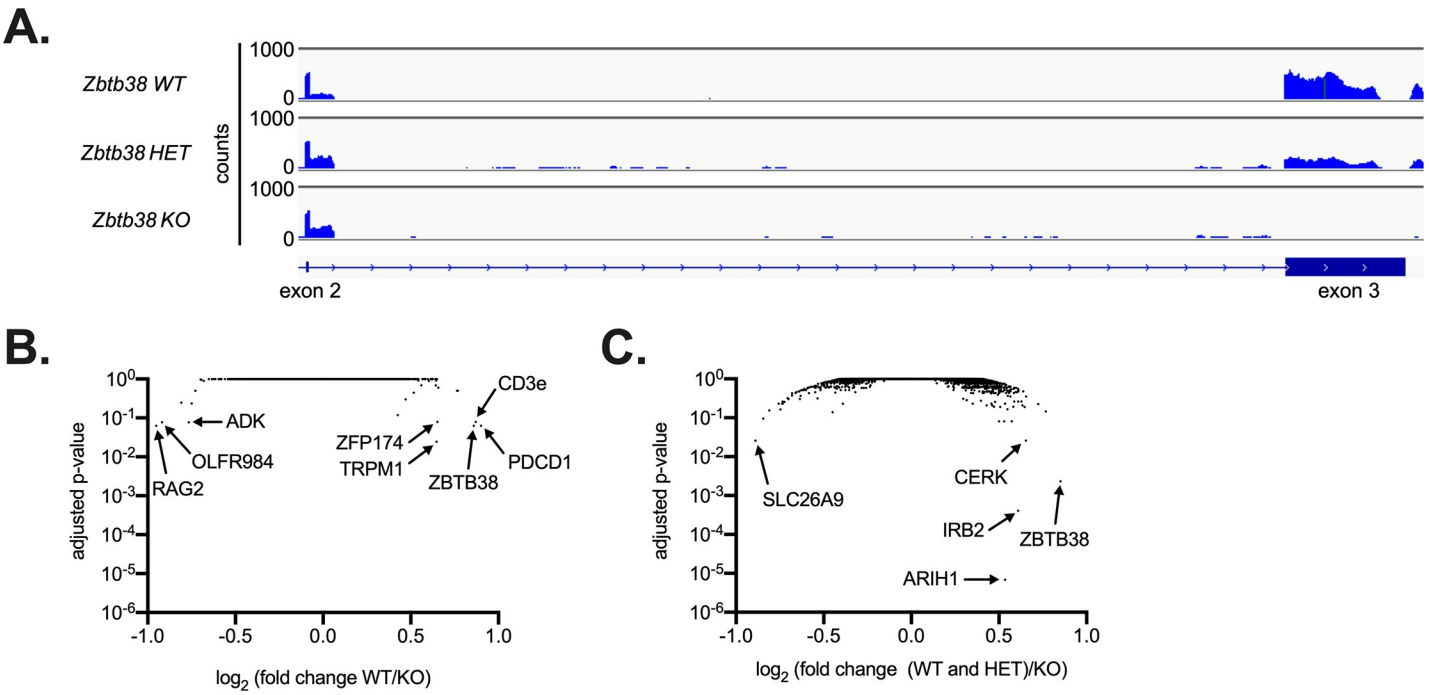

Fig 3. ZBTB38 deficiency minimally impacts gene expression in germinal center B cells. (**A**) RNA-seq reads across exons 2–3 of *Zbtb38*. Paired-end RNA-seq of antigen specific (NP^+) germinal center B cells ($CD19^+GL7^+IgD^-$) from $Zbtb38^{fl/fl}$ (ZBTB38 WT), $Zbtb38^{+/fl}$ *x Vav-Cre* (ZBTB38 HET), and $Zbtb38^{fl/fl}$ *x Vav-Cre* (ZBTB38 KO) mice were aligned to the mm10 mouse genome and shown using IgV browser. One representative trace is shown for each genotype. (**B**) Volcano plot depicting differential gene expression between ZBTB38 WT (n = 2) and ZBTB38 KO (n = 6) mice. Statistically significant genes were determined through DESeq2 and an adjusted p-value of 0.1. (**C**) Differential gene expression between ZBTB38 WT and ZBTB38 HET (n = 4 in total) and ZBTB38 KO (n = 6). Statistically significant genes were determined through DESeq2 and an adjusted p-value of 0.1.

https://doi.org/10.1371/journal.pone.0235183.g003

controls that lack Cre recombinase (ZBTB38 WT). We next used Salmon to quantify transcript abundances and DESeq2 to identify genes differentially expressed between ZBTB38-deficient mice and controls [29, 30]. Other than ZBTB38 itself, very few genes were dysregulated in ZBTB38-deficient cells (Fig 3B; S1 Table). To increase statistical power, we compared ZBTB38-deficient samples to both wild-type and heterozygous controls. Again, very few differences were observed (Fig 3C; S2 Table). The few dysregulated genes were expressed at very low levels (e.g. CD3e) across genotypes and did not to fall into any obvious pathways or signatures.

ZBTB38 deficiency does not impair B cell responses

To determine if ZBTB38 expression is important for B cell development, we examined the frequency of B cell subsets in ZBTB38 WT and ZBTB38 KO mice. ZBTB38 deficiency did not alter the frequencies of follicular (FoB, $CD11b^-CD19^+IgD^+IgM^+$), marginal zone (MZ, $CD11b^-CD19^+CD93^-CD21^+CD23^-$), T1 transitional ($CD11b^-CD19^+CD93^+$,$CD23^-$), T2/3 transitional ($CD11b^-CD19^+CD93^+$,$CD23^+$), isotype-switched memory B cells (swIg MBCs, $CD19^+IgM^-IgD^-CD80^+CCR6^+$), or total splenocyte numbers (S2A Fig). Bone marrow cellularity and plasma cell numbers in unimmunized mice were also similar across genotypes (S2B Fig).

Deficiencies in two other BTB-ZF factors, ZBTB20 and ZBTB32, do not impair B cell development at steady state but cause profound effects on plasma cell lifespan despite modest changes in gene expression [10–13]. These differences are most pronounced in specific immunization conditions and are not readily apparent in polyclonal populations of unimmunized animals. Therefore, to determine if ZBTB38 has a functional role in primary B cell responses,

we first examined GC reactions. We immunized ZBTB38 WT and KO mice with NP-OVA and quantified the frequency of NP-specific GC B cells 2 weeks later, which corresponds with peak GC reactions [38]. We observed no differences in the frequencies of NP-specific GC B cells between ZBTB38 WT and KO mice (Fig 4A; S2C and S2D Fig). NP-specific serum antibodies were also similar between ZBTB38 WT and KO mice at all time points measured (Fig 4B). To specifically quantify the level of high affinity antibodies in the serum by ELISA, low density antigen (NP_4) was used to probe for antibody binding. Low density NP (NP_4) is used to capture antibodies with slow off-rates, which is correlated with antigen high affinity. This contrasts with high density NP (NP_{16}), which can capture antibodies with faster off rates due to the increased concentration of antigen. Unlike the total levels of NP-specific antibodies over time, which plateaued two weeks after immunization, the concentration of high affinity antibodies increased steadily over time and plateaued four weeks after immunization (Fig 4C). No difference in the quantity of high affinity antibodies was observed between ZBTB38 WT and KO mice (Fig 4C). Furthermore, the extent of affinity maturation, quantified as the ratio of

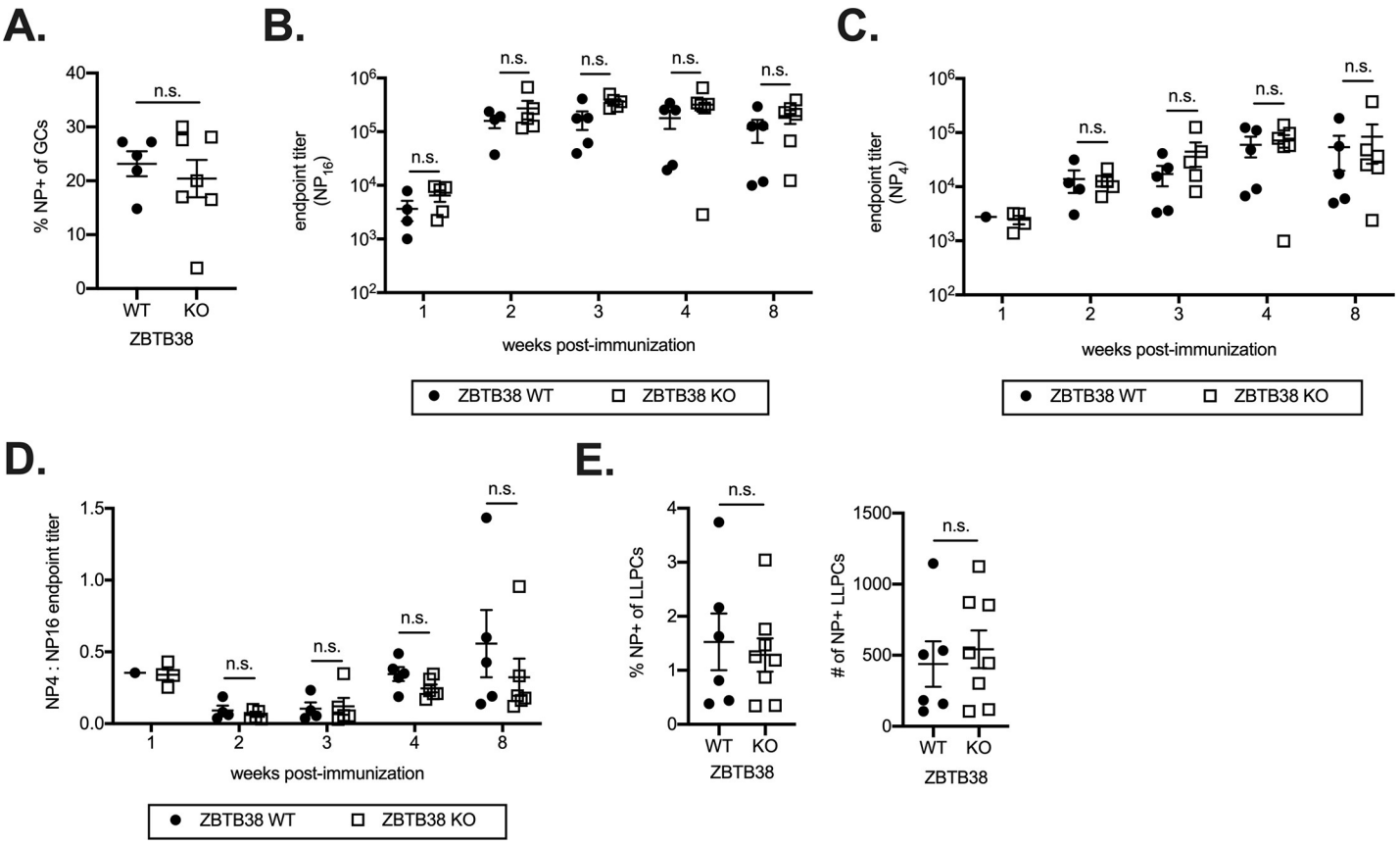

Fig 4. ZBTB38 is dispensable for primary B cell responses. (**A**) ZBTB38 WT and KO mice were immunized with NP-OVA and the frequency of NP-specific germinal center B cells two weeks post immunization was quantified by flow cytometry. Example NP-staining for GC B cells is shown in S2B. Mean ± SEM are shown; each symbol represents an individual mouse. Statistical significance was calculated by Mann-Whitney test; n.s. = not significant ($p > 0.05$). (**B, C**) ZBTB38 WT and KO mice were immunized with NP-OVA and total serum antibody titers (**B**) and high affinity serum antibody titers (**C**) to NP were quantified by ELISA. Endpoint titers are calculated as the reciprocal serum dilution that was three standard deviations above background. Mean ± SEM are shown; each symbol represents an individual mouse. Statistical significance was calculated by Mann-Whitney test for each timepoint; n.s. = not significant ($p > 0.05$). (**D**) Affinity maturation of the antibodies was calculated as the ratio of endpoint titers to NP4: NP16 and plotted at each time point for ZBTB38 WT and ZBTB38 KO mice. Mean ± SEM are shown; each symbol represents an individual mouse. Statistical significance was calculated by Mann-Whitney test for each timepoint; n.s. = not significant ($p > 0.05$). (**E**) The frequency and number of NP-specific long-lived plasma cells was calculated by flow cytometry. Long-lived plasma cells were analyzed 8 weeks post-NP immunization. Gating strategies are shown in S2C Fig. Mean ± SEM are shown; each symbol represents an individual mouse. Statistical significance was calculated by Mann-Whitney test for each timepoint; n.s. = not significant ($p > 0.05$).

https://doi.org/10.1371/journal.pone.0235183.g004

NP_4 to NP_{16} endpoint titers, was similar between ZBTB38 WT and KO mice (Fig 4D). Finally, we observed similar numbers and frequencies of antigen-specific bone marrow plasma cells (Fig 4E, S2E Fig).

Possible explanations for the similar serum antibody levels in ZBTB38 WT and KO mice include similar frequencies of antigen-specific LLPCs or compensatory increased antibody secretion from fewer LLPCs. To differentiate between these two possibilities, the frequency of NP-specific LLPCs was quantified by flow cytometry 8 weeks after alhydrogel-adjuvanted NP-OVA immunization of ZBTB38 WT and KO mice. The frequency and number of NP-specific LLPCs was similar between ZBTB38 WT and KO mice (Fig 4E; S2E Fig). These data demonstrate that ZBTB38 is dispensable for primary antibody responses to hapten-protein antigens.

To determine if ZBTB38 expression is required for secondary responses and MBC differentiation, the frequency of NP-specific memory B cells ($CD19^+GL7^-IgM^-IgD^-CD80^+CCR6^+$) was quantified in ZBTB38 WT and KO mice 8 weeks after immunization with alhydrogel-adjuvanted NP-OVA. No difference was observed in the frequency or number of NP-specific MBCs (Fig 5A; S3 Fig). To assess MBC function, splenocytes from ZBTB38 WT and KO mice were adoptively transferred into allotype-distinct naïve IgH^a recipients and mice challenged with soluble NP-OVA 24 hours later. Donor IgH^b NP-specific antibodies originating from ZBTB38 WT and KO mice were tracked over time. NP-specific antibody titers were not altered by ZBTB38 deficiency (Fig 5B). Thus, ZBTB38 is also dispensable for secondary B cell responses.

ZBTB38 deficiency does not alter the development of hematopoietic cells

Given ZBTB38 expression in hematopoietic progenitors (Fig 1A), we next assessed if ZBTB38 deficiency alters the development of lymphoid and/or myeloid lineages by quantifying the frequencies of different cell populations by flow cytometry. We first focused on hematopoietic stem cells (HSCs, $cKit^+Sca1^+Flk2^-CD27^+$) and progenitors with varying degrees of lineage commitment in the bone marrow [39]. HSCs differentiate into multipotent progenitors

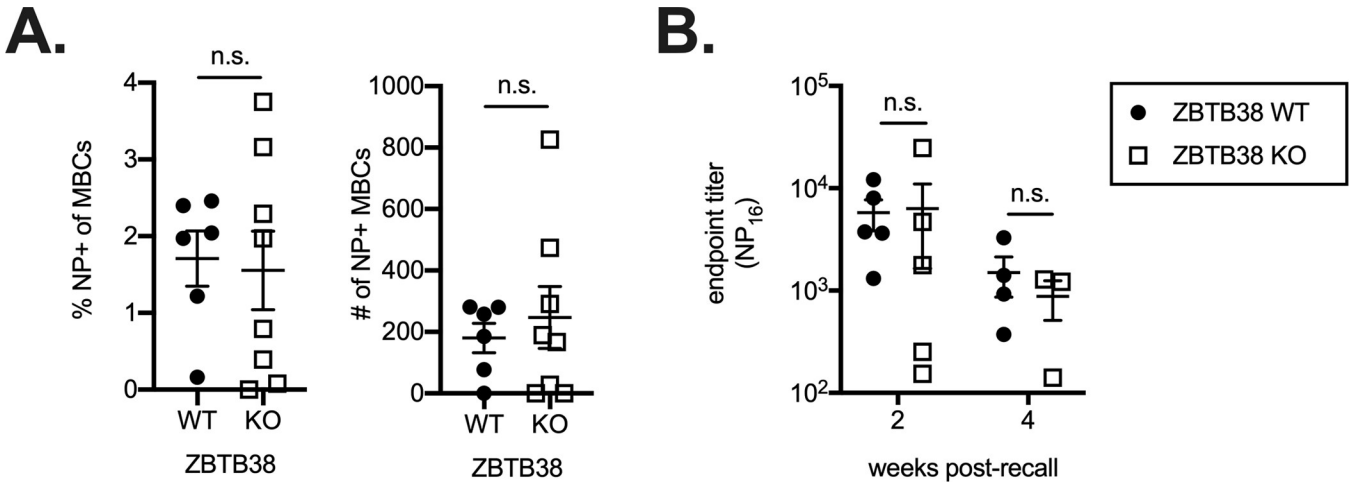

Fig 5. Memory B cell responses do not require ZBTB38. (**A**) The frequency of NP-specific memory B cells ($CD19^+GL7^-IgM^-IgD^-CD80^+CCR6^+$) was quantified by flow cytometry in ZBTB38 WT and KO mice 8 weeks after NP-OVA immunization. Gating strategies are shown in S3 Fig. Mean ± SEM are shown; each symbol represents an individual mouse. Statistical significance was calculated by Mann-Whitney test; n.s. = not significant ($p > 0.05$). (**B**) Splenocytes from ZBTB38 WT and ZBTB38 KO mice were adoptively transferred into IgH^a naïve hosts and challenged with soluble NP-OVA one day after transfer. Donor (IgH^b) antibody responses were calculated as the endpoint titer against high density NP. Mean ± SEM are shown; each symbol represents an individual mouse. Statistical significance was calculated by Mann-Whitney test for each timepoint; n.s. = not significant ($p > 0.05$).

https://doi.org/10.1371/journal.pone.0235183.g005

(MPPs, cKit$^+$Sca1$^+$Flk2$^+$CD27$^+$) that can give rise to both the myeloid and lymphoid lineages. MPPs can then differentiate into common myeloid progenitors (CMPs, cKit$^+$Sca1$^-$Flk2$^+$FcγR$^-$) or common lymphoid progenitors (CLPs, cKit$^{-/lo}$Sca1$^-$CD27$^+$FcγR$^-$Flk2$^+$IL7Rα$^+$) [40, 41]. CLPs give rise to B, T, natural killer (NK), and innate like cells (ILCs). CMPs give rise to basophils, eosinophils, mast cells, dendritic cells as well as granulocyte monocyte progenitors (GMPs, cKit$^+$Sca1$^-$Flk2$^-$FcγR$^+$) [41]. GMPs can then give rise to neutrophils and monocytes. We identified no statistically significant differences in the frequencies of these progenitor populations between ZBTB38 WT and KO mice (Fig 6A; S4 Fig).

Mean ± SEM are shown; each symbol represents an individual mouse. Statistical significance was determined by Mann-Whitney test; n.s. indicates no significance ($p > 0.05$). (**B**) Frequencies of B cells (B220$^+$), natural killer (NK, NK1.1$^+$) cells, CD4$^+$ and CD8$^+$ T cells (B220$^-$CD11b$^-$NK.1$^-$), monocytes (CD11b$^+$Ly6C^{hi}Ly6G$^-$), and neutrophils (CD11b$^+$Ly6-C$^+$Ly6G$^+$) of peripheral blood mononuclear cells (PBMCs) from ZBTB38 WT and KO mice were quantified by flow cytometry. Mean ± SEM are shown; each symbol represents an individual mouse. Statistical significance was determined by Mann-Whitney test; n.s. indicates no significance ($p > 0.05$).

To assess if mature hematopoietic lineages require ZBTB38 for their development or maintenance, we analyzed the frequencies of different peripheral blood mononuclear cell (PBMCs) populations. We observed no differences between ZBTB38 WT and KO mice in the frequencies of B cells (B220$^+$), NK cells (NK1.1$^+$), T (CD4$^+$ or CD8$^+$ B220$^-$NK1.1$^-$CD11b$^-$), monocytes (CD11b$^+$Ly6C^{hi}Ly6G$^-$), or neutrophils (CD11b$^+$Ly6C$^+$Ly6G$^+$) (Fig 6B). Thus, ZBTB38 is not required for the development or maintenance of these hematopoietic lineages.

Discussion

BTB-ZF family members such as BCL-6, ZBTB32, and ZBTB20, have critical roles in different aspects of B cell responses. ZBTB38, another member of the BTB-ZF family, has been implicated in DNA damage responses and replication efficiency. This occurs through repression of MCM10 expression, and potentially binding of other methylated CpG sites throughout the

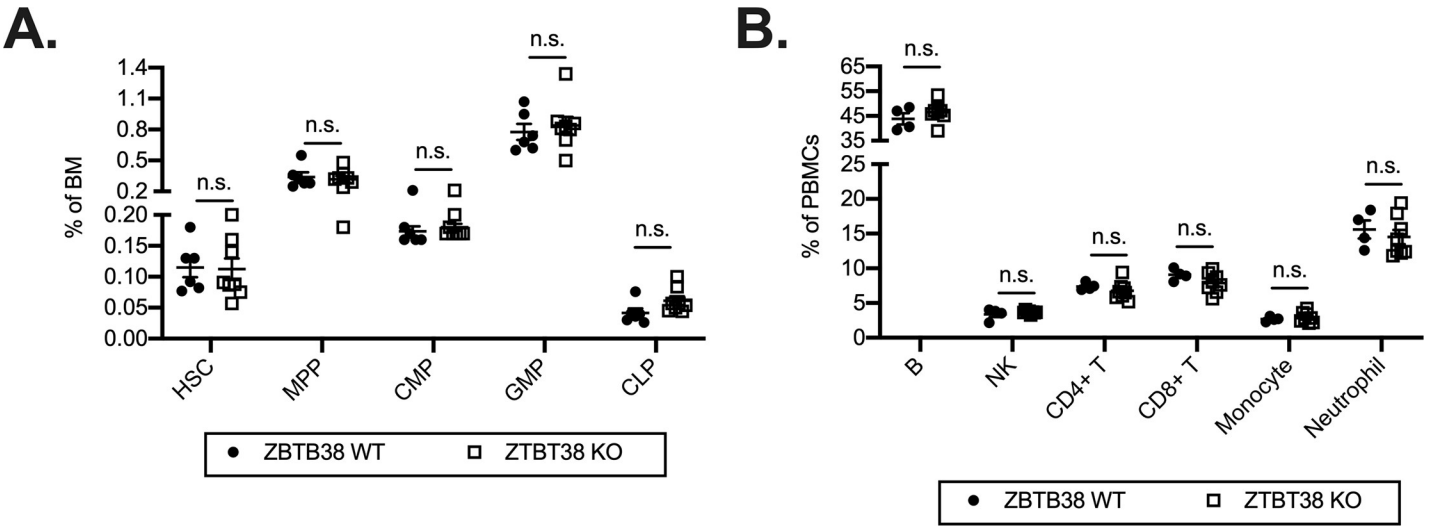

Fig 6. ZBTB38 deficiency does not impact hematopoietic development of maintenance. (**A**) Frequencies of hematopoietic stem cells (HSCs, cKit$^+$Sca1$^+$Flk2$^-$CD27$^+$), multi-potent progenitors (MPPs, cKit$^+$Sca1$^+$Flk2$^+$CD27$^+$), common myeloid progenitors (CMPs, cKit$^+$Sca1$^-$Flk2$^+$FcγR$^-$), granulocyte monocyte progenitors (GMPs, cKit$^+$Sca1$^-$Flk2$^-$FcγR$^+$), and common lymphoid progenitors (CLPs, cKit$^{-/lo}$Sca1$^-$CD27$^+$FcγR$^-$Flk2$^+$IL7Rα$^+$) in the bone marrow from ZBTB38 WT and KO mice were quantified by flow cytometry. Gating strategies are shown in S4 Fig.

https://doi.org/10.1371/journal.pone.0235183.g006

genome [18, 20]. Replication fidelity and DNA damage responses are key processes during germinal center reactions, as B cells accumulate somatic mutations and undergo dsDNA breaks as part of immunoglobulin isotype switching [42]. Yet our data demonstrate that ZBTB38 is dispensable for both primary and recall B cell responses to model T-dependent antigens despite high levels of expression in both germinal center B cells and antibody-secreting plasma cells. Our data do not preclude the possibility that ZBTB38 is important for T-independent antigens or other forms of T-dependent responses. For example, prior studies by our group demonstrated that ZBTB20 is required for alum-adjuvanted responses, but not when using other adjuvants [10]. In addition, other Cre drivers that promote deletion only in activated B cells may be preferable to the pan-hematopoietic deletion system we employed here.

ZBTB38 is also dispensable for maintaining homeostasis of lymphoid and myeloid hematopoietic lineages. Thus, the evolutionary and functional reasons why ZBTB38 is expressed in the hematopoietic and immune system are not fully resolved. Instead, the most important roles for ZBTB38 may lie in other cell types, tissues, and/or physiological contexts. Genome-wide association studies in humans have identified single nucleotide polymorphisms (SNPs) in ZBTB38 that are associated with shorter stature in Chinese populations but taller stature in Korean populations [34–36, 43]. However, when *Zbtb38* f/f mice were crossed to CMV-Cre expressing mice, germline deletion of ZBTB38 did not result in observable differences in the length or weight of the mice. Further characterization of how SNPs influence ZBTB38 function, and identifying the location of SNPs, may provide further explanation of why certain polymorphisms are associated with altered height.

ZBTB38 deletion or knockdown has resulted in impaired cellular processes in neuronal injuries or tumors. For instance, increasing ZBTB38 expression reduces apoptosis and promotes autophagy in a spinal cord injury model, and results in increased neuronal repair [25, 44, 45]. In contrast, ZBTB38 expression has been shown to promote proliferation and differentiation of a neuroblastoma cell line [46]. These differences in the functional roles of ZBTB38 may be attributed to subtype-specific sensitivity of neurons to oxidative stress [47]. ZBTB38, along with USP9X, a deubiquitinase, is required to limit basal reactive oxidative species (ROS) levels and the response to oxidative stress [48]. Given the high levels of ZBTB38 expression in neurons, perhaps ZBTB38 is involved with balancing neuronal death with recovery after various challenges. Neuronal insult, such as injury, stroke, or cancer may be necessary to identify processes regulated by ZBTB38. We did not observe any obviously altered behaviors in our animals, though this would require more in-depth experimentation by experts. Future studies focused on such other cell types and systems will be facilitated by the novel *Zbtb38* f/f mice that we have generated.

Supporting information

S1 Fig. Gating strategy for naïve B cells, splenic plasma cells, light zone germinal center B cells, and dark zone germinal center B cells. Flow cytometric gating strategies for NP-specific splenic plasma cell (SpPC), light zone (LZ) and dark zone (DZ) germinal center (GC) B cells shown in Fig 1B.
(TIFF)

S2 Fig. Gating strategy for long-lived plasma cells. (A) Frequencies of follicular (FoB, $CD11b^{-}CD19^{+}IgD^{+}IgM^{+}$), marginal zone (MZ, $CD11b^{-}CD19^{+}CD93^{-}CD21^{+}CD23^{-}$), T1 transitional ($CD11b^{-}CD19^{+}CD93^{+},CD23^{-}$), T2/3 transitional ($CD11b^{-}CD19^{+}CD93^{+},CD23^{+}$), isotype-switched memory B cells (swIg MBCs, $CD19^{+}IgM^{-}IgD^{-}CD80^{+}CCR6^{+}$), and bone marrow plasma cells ($B220^{-}CD138^{+}$) at steady state for ZBTB38 WT and ZBTB38 KO mice. Total numbers of splenocytes are shown in the right panel. Mean ± SEM are shown; each symbol

represents an individual mouse. Statistical significance was calculated by Mann-Whitney test; n.s. = not significant ($p > 0.05$). (B) Frequencies of bone marrow plasma cells (left panel) and total numbers of bone marrow cells (right panel) are shown across genotypes. Statistical significance was calculated by Mann-Whitney test; n.s. = not significant ($p > 0.05$). (C) Germinal center (CD19+ GL7+) frequency after magnetic bead enrichment for GL7-expressing splenocytes. Statistical significance was calculated by Mann-Whitney test; n.s. = not significant ($p > 0.05$). (D) Concatenated flow plots of NP+ germinal center B cells ($CD19^+GL7^+IgD^-$) for ZBTB38 WT (n = 3) and ZBTB38 KO (n = 2) mice. (E) Flow cytometric gating strategy for NP-specific long-lived plasma cells (LLPCs) in the bone marrow.
(TIFF)

S3 Fig. Gating strategy for isotype-switched memory B cells. Flow cytometric gating strategy for NP-specific, isotype-switched memory B cells (swIg MBCs) in the spleen. Cells were gated on $CD19^+GL7^-$.
(TIFF)

S4 Fig. Gating strategy for bone marrow progenitors. Flow cytometric gating strategies for bone marrow progenitors shown in Fig 6A. HSC, hematopoietic stem cell; MPP, multi-potent progenitor; CMP, common myeloid progenitor; GMP, granulocyte monocyte progenitor; CLP, common lymphoid progenitor.
(TIFF)

S1 File.
(PDF)

S1 Table. Differentially-expressed genes between ZBTB38-deficient and -sufficient germinal center B cells.
(XLSX)

S2 Table. Differentially-expressed genes in ZBTB38-deficient vs. heterozygous and -sufficient germinal center B cells.
(XLSX)

Acknowledgments

The authors thank M. White in the Transgenic and Knockout Mouse Core at Washington University for assistance with microinjections. Flow cytometry experiments reported in this publication were supported by Flow Cytometry and Fluorescence Activated Cell Sorting Core at Washington University in St. Louis.

Author Contributions

Conceptualization: Rachel Wong, Deepta Bhattacharya.

Data curation: Deepta Bhattacharya.

Formal analysis: Deepta Bhattacharya.

Funding acquisition: Deepta Bhattacharya.

Investigation: Rachel Wong, Deepta Bhattacharya.

Methodology: Rachel Wong.

Supervision: Deepta Bhattacharya.

Writing – original draft: Rachel Wong.

Writing – review & editing: Rachel Wong, Deepta Bhattacharya.

References

1. De Silva NS, Klein U. Dynamics of B cells in germinal centres. Nat Rev Immunol. 2015; 15(3):137–48. Epub 2015/02/07. https://doi.org/10.1038/nri3804 PMID: 25656706; PubMed Central PMCID: PMC4399774.
2. Roco JA, Mesin L, Binder SC, Nefzger C, Gonzalez-Figueroa P, Canete PF, et al. Class-Switch Recombination Occurs Infrequently in Germinal Centers. Immunity. 2019; 51(2):337–50 e7. Epub 2019/08/04. https://doi.org/10.1016/j.immuni.2019.07.001 PMID: 31375460; PubMed Central PMCID: PMC6914312.
3. Purtha WE, Tedder TF, Johnson S, Bhattacharya D, Diamond MS. Memory B cells, but not long-lived plasma cells, possess antigen specificities for viral escape mutants. Journal of Experimental Medicine. 2011; 208:2599–606. Epub 2011/12/14. https://doi.org/10.1084/jem.20110740 PMID: 22162833.
4. Chevrier S, Corcoran LM. BTB-ZF transcription factors, a growing family of regulators of early and late B-cell development. Immunology and cell biology. 2014; 92:481–8. https://doi.org/10.1038/icb.2014.20 PMID: 24638067.
5. Dhordain P, Albagli O, Lin RJ, Ansieau S, Quief S, Leutz A, et al. Corepressor SMRT binds the BTB/POZ repressing domain of the LAZ3/BCL6 oncoprotein. Proc Natl Acad Sci U S A. 1997; 94 (20):10762–7. https://doi.org/10.1073/pnas.94.20.10762 PMID: 9380707.
6. Dhordain P, Lin RJ, Quief S, Lantoine D, Kerckaert JP, Evans RM, et al. The LAZ3(BCL-6) oncoprotein recruits a SMRT/mSIN3A/histone deacetylase containing complex to mediate transcriptional repression. Nucleic Acids Res. 1998; 26(20):4645–51. https://doi.org/10.1093/nar/26.20.4645 PMID: 9753732.
7. Hong SH, David G, Wong CW, Dejean A, Privalsky ML. SMRT corepressor interacts with PLZF and with the PML-retinoic acid receptor alpha (RARalpha) and PLZF-RARalpha oncoproteins associated with acute promyelocytic leukemia. Proc Natl Acad Sci U S A. 1997; 94(17):9028–33. https://doi.org/10.1073/pnas.94.17.9028 PMID: 9256429.
8. Wong C-W, Privalsky ML. Components of the SMRT Corepressor Complex Exhibit Distinctive Interactions with the POZ Domain Oncoproteins PLZF, PLZF-RARα, and BCL-6. Journal of Biological Chemistry. 1998; 273(42):27695–702. https://doi.org/10.1074/jbc.273.42.27695 PMID: 9765306
9. Ye BH, Cattoretti G, Shen Q, Zhang J, Hawe N, Waard Rd, et al. The BCL-6 proto-oncogene controls germinal-centre formation and Th2-type inflammation. Nature Genetics. 1997; 16(2):161–70. https://doi.org/10.1038/ng0697-161 PMID: 9171827
10. Wang Y, Bhattacharya D. Adjuvant-specific regulation of long-term antibody responses by ZBTB20. The Journal of Experimental Medicine. 2014; 211(5):841. https://doi.org/10.1084/jem.20131821 PMID: 24711582
11. Chevrier S, Emslie D, Shi W, Kratina T, Wellard C, Karnowski A, et al. The BTB-ZF transcription factor Zbtb20 is driven by Irf4 to promote plasma cell differentiation and longevity. The Journal of Experimental Medicine. 2014; 211(5):827. https://doi.org/10.1084/jem.20131831 PMID: 24711583
12. Jash A, Wang Y, Weisel FJ, Scharer CD, Boss JM, Shlomchik MJ, et al. ZBTB32 Restricts the Duration of Memory B Cell Recall Responses. J Immunol. 2016; 197:1159–68. Epub 2016/07/01. https://doi.org/10.4049/jimmunol.1600882 PMID: 27357154.
13. Jash A, Zhou YW, Gerardo DK, Ripperger TJ, Parikh BA, Piersma S, et al. ZBTB32 restrains antibody responses to murine cytomegalovirus infections, but not other repetitive challenges. Scientific Reports. 2019; 9(1):15257. https://doi.org/10.1038/s41598-019-51860-z PMID: 31649328
14. Ocskó T, Tóth DM, Hoffmann G, Tubak V, Glant TT, Rauch TA. Transcription factor Zbtb38 downregulates the expression of anti-inflammatory IL1r2 in mouse model of rheumatoid arthritis. Biochimica et Biophysica Acta (BBA)—Gene Regulatory Mechanisms. 2018; 1861(11):1040–7. https://doi.org/10.1016/j.bbagrm.2018.09.007.
15. Filion GJP, Zhenilo S, Salozhin S, Yamada D, Prokhortchouk E, Defossez P-A. A family of human zinc finger proteins that bind methylated DNA and repress transcription. Molecular and cellular biology. 2006; 26:169–81. https://doi.org/10.1128/MCB.26.1.169-181.2006 PMID: 16354688.
16. Sasai N, Matsuda E, Sarashina E, Ishida Y, Kawaichi M. Identification of a novel BTB-zinc finger transcriptional repressor, CIBZ, that interacts with CtBP corepressor. Genes to cells: devoted to molecular & cellular mechanisms. 2005; 10:871–85. https://doi.org/10.1111/j.1365-2443.2005.00885.x PMID: 16115196.

17. Sasai N, Nakao M, Defossez P-A. Sequence-specific recognition of methylated DNA by human zinc-finger proteins. Nucleic Acids Res. 2010; 38(15):5015–22. https://doi.org/10.1093/nar/gkq280 PMID: 20403812

18. Hudson NO, Whitby FG, Buck-Koehntop BA. Structural insights into methylated DNA recognition by the C-terminal zinc fingers of the DNA reader protein ZBTB38. J Biol Chem. 2018; 293(51):19835–43. Epub 2018/10/26. https://doi.org/10.1074/jbc.RA118.005147 PMID: 30355731; PubMed Central PMCID: PMC6314133.

19. de Dieuleveult M, Miotto B. DNA Methylation and Chromatin: Role(s) of Methyl-CpG-Binding Protein ZBTB38. Epigenet Insights. 2018; 11:2516865718811117. Epub 2018/11/28. https://doi.org/10.1177/2516865718811117 PMID: 30480223; PubMed Central PMCID: PMC6243405.

20. Miotto B, Chibi M, Xie P, Koundrioukoff S, Moolman-Smook H, Pugh D, et al. The RBBP6/ZBTB38/MCM10 axis regulates DNA replication and common fragile site stability. Cell reports. 2014; 7:575–87. https://doi.org/10.1016/j.celrep.2014.03.030 PMID: 24726359.

21. Oikawa Y, Omori R, Nishii T, Ishida Y, Kawaichi M, Matsuda E. The methyl-CpG-binding protein CIBZ suppresses myogenic differentiation by directly inhibiting myogenin expression. Cell research. 2011; 21:1578–90. https://doi.org/10.1038/cr.2011.90 PMID: 21625269.

22. Nishii T, Oikawa Y, Ishida Y, Kawaichi M, Matsuda E. CtBP-interacting BTB zinc finger protein (CIBZ) promotes proliferation and G1/S transition in embryonic stem cells via Nanog. The Journal of biological chemistry. 2012; 287:12417–24. https://doi.org/10.1074/jbc.M111.333856 PMID: 22315219.

23. Kotoku T, Kosaka K, Nishio M, Ishida Y, Kawaichi M, Matsuda E. CIBZ Regulates Mesodermal and Cardiac Differentiation of by Suppressing T and Mesp1 Expression in Mouse Embryonic Stem Cells. Scientific reports. 2016; 6:34188–. https://doi.org/10.1038/srep34188 PMID: 27659197.

24. Oikawa Y, Matsuda E, Nishii T, Ishida Y, Kawaichi M. Down-regulation of CIBZ, a novel substrate of caspase-3, induces apoptosis. The Journal of biological chemistry. 2008; 283:14242–7. https://doi.org/10.1074/jbc.M802257200 PMID: 18375381.

25. Cai Y, Li J, Yang S, Li P, Zhang X, Liu H. CIBZ, a novel BTB domain-containing protein, is involved in mouse spinal cord injury via mitochondrial pathway independent of p53 gene. PloS one. 2012; 7:e33156. https://doi.org/10.1371/journal.pone.0033156 PMID: 22427977.

26. Chou C, Pinto AK, Curtis JD, Persaud SP, Cella M, Lin C-C, et al. c-Myc-induced transcription factor AP4 is required for host protection mediated by CD8+ T cells. Nature immunology. 2014; 15(9):884–93. Epub 2014/07/13. https://doi.org/10.1038/ni.2943 PMID: 25029552.

27. Kim D, Paggi JM, Park C, Bennett C, Salzberg SL. Graph-based genome alignment and genotyping with HISAT2 and HISAT-genotype. Nat Biotechnol. 2019; 37(8):907–15. Epub 2019/08/04. https://doi.org/10.1038/s41587-019-0201-4 PMID: 31375807.

28. Thorvaldsdottir H, Robinson JT, Mesirov JP. Integrative Genomics Viewer (IGV): high-performance genomics data visualization and exploration. Brief Bioinform. 2013; 14(2):178–92. Epub 2012/04/21. https://doi.org/10.1093/bib/bbs017 PMID: 22517427; PubMed Central PMCID: PMC3603213.

29. Patro R, Duggal G, Love MI, Irizarry RA, Kingsford C. Salmon provides fast and bias-aware quantification of transcript expression. Nat Methods. 2017; 14(4):417–9. Epub 2017/03/07. https://doi.org/10.1038/nmeth.4197 PMID: 28263959; PubMed Central PMCID: PMC5600148.

30. Love MI, Huber W, Anders S. Moderated estimation of fold change and dispersion for RNA-seq data with DESeq2. Genome Biol. 2014; 15(12):550. Epub 2014/12/18. https://doi.org/10.1186/s13059-014-0550-8 PMID: 25516281; PubMed Central PMCID: PMC4302049.

31. Shi W, Liao Y, Willis SN, Taubenheim N, Inouye M, Tarlinton DM, et al. Transcriptional profiling of mouse B cell terminal differentiation defines a signature for antibody-secreting plasma cells. Nature Immunology. 2015; 16(6):663–73. https://doi.org/10.1038/ni.3154 PMID: 25894659

32. Heng TS, Painter MW, Immunological Genome Project C. The Immunological Genome Project: networks of gene expression in immune cells. Nat Immunol. 2008; 9(10):1091–4. Epub 2008/09/19. https://doi.org/10.1038/ni1008-1091 PMID: 18800157.

33. Victora GD, Schwickert TA, Fooksman DR, Kamphorst AO, Meyer-Hermann M, Dustin ML, et al. Germinal center dynamics revealed by multiphoton microscopy with a photoactivatable fluorescent reporter. Cell. 2010; 143(4):592–605. Epub 2010/11/16. https://doi.org/10.1016/j.cell.2010.10.032 PMID: 21074050; PubMed Central PMCID: PMC3035939.

34. Gudbjartsson DF, Walters GB, Thorleifsson G, Stefansson H, Halldorsson BV, Zusmanovich P, et al. Many sequence variants affecting diversity of adult human height. Nature Genetics. 2008; 40(5):609–15. https://doi.org/10.1038/ng.122 PMID: 18391951

35. Kim J-J, Park Y-M, Baik K-H, Choi H-Y, Yang G-S, Koh I, et al. Exome sequencing and subsequent association studies identify five amino acid-altering variants influencing human height. Human Genetics. 2012; 131(3):471–8. https://doi.org/10.1007/s00439-011-1096-4 PMID: 21959382

36. Wang Y, Wang Z-m, Teng Y-c, Shi J-x, Wang H-f, Yuan W-t, et al. An SNP of the ZBTB38 gene is associated with idiopathic short stature in the Chinese Han population. Clinical Endocrinology. 2013; 79 (3):402–8. https://doi.org/10.1111/cen.12145 PMID: 23302005

37. Georgiades P, Ogilvy S, Duval H, Licence DR, Charnock-Jones DS, Smith SK, et al. VavCre transgenic mice: a tool for mutagenesis in hematopoietic and endothelial lineages. Genesis. 2002; 34(4):251–6. Epub 2002/11/16. https://doi.org/10.1002/gene.10161 PMID: 12434335.

38. Weisel FJ, Zuccarino-Catania GV, Chikina M, Shlomchik MJ. A Temporal Switch in the Germinal Center Determines Differential Output of Memory B and Plasma Cells. Immunity. 2016; 44:116–30. https://doi.org/10.1016/j.immuni.2015.12.004 PMID: 26795247.

39. Spangrude GJ, Heimfeld S, Weissman IL. Purification and characterization of mouse hematopoietic stem cells. Science. 1988; 241(4861):58. https://doi.org/10.1126/science.2898810 PMID: 2898810

40. Kondo M, Weissman IL, Akashi K. Identification of Clonogenic Common Lymphoid Progenitors in Mouse Bone Marrow. Cell. 1997; 91(5):661–72. https://doi.org/10.1016/s0092-8674(00)80453-5 PMID: 9393859

41. Akashi K, Traver D, Miyamoto T, Weissman IL. A clonogenic common myeloid progenitor that gives rise to all myeloid lineages. Nature. 2000; 404(6774):193–7. https://doi.org/10.1038/35004599 PMID: 10724173

42. Phan RT, Dalla-Favera R. The BCL6 proto-oncogene suppresses p53 expression in germinal-centre B cells. Nature. 2004; 432(7017):635–9. Epub 2004/12/04. https://doi.org/10.1038/nature03147 PMID: 15577913.

43. Cho YS, Go MJ, Kim YJ, Heo JY, Oh JH, Ban H-J, et al. A large-scale genome-wide association study of Asian populations uncovers genetic factors influencing eight quantitative traits. Nature Genetics. 2009; 41(5):527–34. https://doi.org/10.1038/ng.357 PMID: 19396169

44. Cai Y, Li J, Zhang Z, Chen J, Zhu Y, Li R, et al. Zbtb38 is a novel target for spinal cord injury. Oncotarget. 2017; 8(28).

45. Chen J, Yan L, Wang H, Zhang Z, Yu D, Xing C, et al. ZBTB38, a novel regulator of autophagy initiation targeted by RB1CC1/FIP200 in spinal cord injury. Gene. 2018; 678:8–16. https://doi.org/10.1016/j.gene.2018.07.073 PMID: 30075197

46. Chen J, Xing C, Yan L, Wang Y, Wang H, Zhang Z, et al. Transcriptome profiling reveals the role of ZBTB38 knock-down in human neuroblastoma. PeerJ. 2019; 7:e6352. https://doi.org/10.7717/peerj.6352 PMID: 30697495

47. Wang X, Michaelis E. Selective neuronal vulnerability to oxidative stress in the brain. Frontiers in Aging Neuroscience. 2010; 2(12). https://doi.org/10.3389/fnagi.2010.00012 PMID: 20552050

48. Miotto B, Marchal C, Adelmant G, Guinot N, Xie P, Marto JA, et al. Stabilization of the methyl-CpG binding protein ZBTB38 by the deubiquitinase USP9X limits the occurrence and toxicity of oxidative stress in human cells. Nucleic Acids Res. 2018; 46(9):4392–404. https://doi.org/10.1093/nar/gky149 PMID: 29490077.